A Tool Path Modification Approach to Cutting Engagement Regulation for the Improvement of Machining Accuracy in 2D Milling With a Straight End Mill

M. Sharif Uddin

Soichi Ibaraki[1]
e-mail: ibaraki@prec.kyoto-u.ac.jp

Atsushi Matsubara

Department of Micro Engineering,
Kyoto University,
Sakyo-Ku, Kyoto 606-8501, Japan

Susumu Nishida
Manufacturing Technology Institute Inc.,
Ebisu 1-19-19, Shibuya-ku,
Tokyo150-0013, Japan
e-mail: nishida@mtii.jp

Yoshiaki Kakino
Kakino Research Institute,
Enpukuji-cho 324-1, Nakagyo-ku,
Kyoto 604-8175, Japan
e-mail: kakino@crux.ocn.ne.jp

In two-dimensional (2D) free-form contour machining by using a straight (flat) end mill, conventional contour parallel paths offer varying cutting engagement with workpiece, which inevitably causes the variation in cutting loads on the tool, resulting in geometric inaccuracy of the machined workpiece surface. This paper presents an algorithm to generate a new offset tool path, such that the cutting engagement is regulated at a desired level over the finishing path. The key idea of the proposed algorithm is that the semi-finish path, the path prior to the finishing path, is modified such that the workpiece surface generated by the semi-finish path gives the desired engagement angle over the finishing path. The expectation with the proposed algorithm is that by regulating the cutting engagement angle along the tool path trajectory, the cutting force can be controlled at any desirable value, which will potentially reduce variation of tool deflection, thus improving geometric accuracy of machined workpiece. In this study, two case studies for 2D contiguous end milling operations with a straight end mill are shown to demonstrate the capability of the proposed algorithm for tool path modification to regulate the cutting engagement. Machining results obtained in both case studies reveal far reduced variation of cutting force, and thus, the improved geometric accuracy of the machined workpiece contour. [DOI: 10.1115/1.2752526]

Keywords: contour parallel path, cutting engagement angle, tool path modification, cutting force, machined surface geometric error, contour end milling

1 Introduction

With the recent advances in high-speed machining technology, 2.5D contour end milling has gained an increasing demand in manufacturing die and mold products. This is partially due to the fact that a surprisingly large number of mechanical parts are made of 2.5D contour and even more complex objects are generally created from a billet by using 2.5D roughing, semi-finishing and finishing. In 2.5D contour machining, conventional tool path patterns generated by commercial CAM (computer-aided manufacturing) software are mostly either direction parallel paths or contour parallel offset paths. In particular, contour parallel offset (CPO) path, which is generated by successive offsets of the input boundary, has been extensively adopted in contour machining. Recently, many numerically robust and efficient algorithms have been developed to generate contour parallel offset paths for any given contour geometries and adopted in commercial CAM software.

During actual contour machining, these conventional contour parallel paths create some cutting problems. To be noted among them is significantly varying cutting engagement that causes the variations in cutter load and tool deflection, and consequently, geometric inaccuracy on machined surface [1]. Also the variations in cutting engagement angle are a significant concern from a process stability and efficiency perspective. Research has already been done to observe this varying cutting engagement [2,3] and to address its inevitable negative consequence resulted from machining with contour parallel paths [4,5]. Shown in Fig. 1 is how the cutting engagement angle varies depending on the geometry of the tool path in the two-dimensional (2D) machining. From Fig. 1, it can be realized that the engagement angle varies depending on the curvature of tool path, the step-over distance (i.e., radial depth of cut), and the tool radius. The engagement angle represents the region of contact between the tool and workpiece material in the two-dimensional machining. Consequently, it can be said that the engagement angle is one of dominant process parameters that determines the cutting load on the tool.

Although contour parallel paths inherently offer cutting problems, a need was also felt how to tackle this varying cutting engagement in contour machining. In order to regulate the material removal rate or the cutting force on arbitrary tool paths, major methods reported in the literature are adjusting the feed rate adaptively. Most of feed-rate adaptation schemes found in the literature are adaptive feedback control schemes (e.g., [6,7]). There have been, however, by far not many practical applications of them in the manufacturing industry. The difficulty to implement an accurate, reliable, and economic way to monitor cutting forces in process and to ensure the reliability of the control has prevented feedback control schemes from being widely implemented in industrial applications [8]. A simpler, but more practically feasible way is in an priori adjustment of feed rate on a NC program (e.g., [9–11]). An important prerequisite for applying this approach is the sophisticated servocontroller of NC machine tool that possesses a rapid acceleration and deceleration control mechanism to response to the frequent and quick change of feed rate in actual machining operation. On commercial CNCs, it is often the case

[1]Corresponding author.

Contributed by the Manufacturing Science Division of ASME for publication in the JOURNAL OF MANUFACTURING SCIENCE AND ENGINEERING. Manuscript received May 1, 2006; final manuscript received March 27, 2007. Review conducted by William J. Endres.

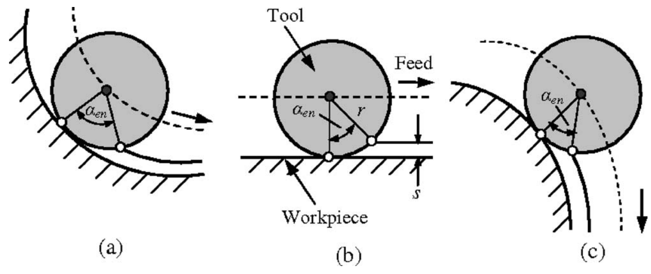

Fig. 1 Variation of cutting engagement angle with respect to different tool path geometry in 2D end milling (r=tool radius, α_{en}=engagement angle, s=step-over distance (i.e., radial depth of cut)): (*a*) concave arc, (*b*) linear, and (*c*) convex arc

that the feed-rate tracking performance is sacrificed in order to secure the contouring accuracy under the prescribed tolerance. Because of this sort of uncertainty in feed-rate control performance, it is often difficult to apply a feed-rate adaptation scheme on a finishing path, where unsmooth or abrupt transient change in feed rate often deteriorates the surface finish.

From this aspect, in order to improve the geometric accuracy of the finished surface by suppressing varying cutting loads, the modification of tool path is more promising. For example, some researchers proposed an attempt to minimize the cutting load when cutting corner regions by applying additional looping tool paths at the corners [12–15]. Their method is an effective ad hoc way to avoid an abrupt and large increase in the cutting force at sharp convex corners, which often becomes a potential cause of the tool damage, by reducing the radial depth of cut there. It is, however, intended to apply only to sharp corners to avoid an abrupt large increase of cutting forces there; it is not intended to apply to continuously regulate the engagement angle on an arbitrary curve.

Stori and Wright [16] proposed a notable approach to offset tool path modification for keeping constant engagement on a tool path of a convex geometry. The key focus of their approach to offset tool path modification can be briefly illustrated in Fig. 2. As can be seen in Fig. 2, for a given original tool center trajectory, $\mathbf{o_k}(i) \in R^2(\mathrm{i}=1,\ldots,N_k)$ and a trajectory of semi-finish surface, $\mathbf{p_k}(i)$, at each step, the algorithm basically aims to shift the tool center location, $\mathbf{o_k}(i)$, by a distance of $x(i)$ to the direction normal to the original tool path such that the engagement angle, $\alpha_{en}(i)$, is regulated to the desirable constant level, α^*_{en}. However, since the algorithm modifies the final path trajectory (i.e., finishing path) to keep constant engagement on it, the modified tool path no longer removes required geometry, leaving excess material in corner cutting. Hence, although this approach may be justified in the application to roughing by spiral-in paths, where efficient material removal is of sole interest, it is practically not possible to be applied to a finishing process. Later, Wang et al. [17] proposed a quantifiable metric-based approach to 2D tool path optimization by considering instantaneous path curvature and cutter engagement. Similarly, their approach would also be effectively realized mainly for a high-speed and stable steady-state roughing operation, but not for a finishing process.

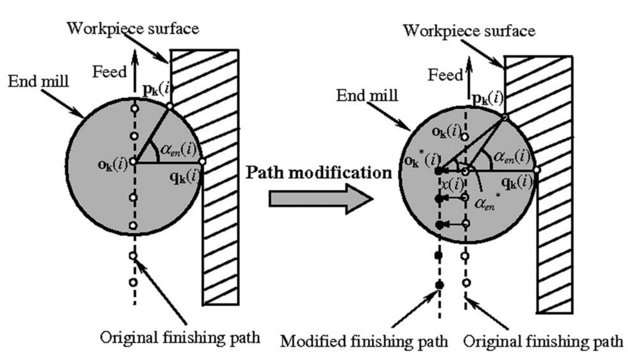

Fig. 2 Simplified illustration of path modification to regulate engagement angle by algorithm introduced by Stori and Wright [16]

In this paper, we propose an algorithm to generate a new offset tool path trajectory, which will regulate cutting engagement at a desired value on the finishing path. Unlike the approach by Stori and Wright [16], the inherent idea of the proposed algorithm is to modify the previous tool path trajectory (i.e., semi-finishing path) with an aim that a desired cutting engagement angle is regulated on the machining with the final path while the geometry of the final path itself is preserved. While approaches available in the literature as described above have focused on mostly stable roughing operation, the proposed algorithm mainly deals with efficient finishing operation in order to produce an improved geometric accuracy and surface quality of the final machined contour.

In this study, the capability of the proposed algorithm for tool path modification is demonstrated to the case with constant engagement angle regulation, and to the case with a feed-rate control scheme where a constant feed rate at the cutting point is maintained. By using a straight end mill, cutting experiments on the core workpiece of hardened steel are carried out to verify the significance of the proposed approach. Results obtained from the experimental verification over conventional contour paths for both cases reveal far reduced variation of cutting force and, hence, an improved geometric accuracy of the machined surface.

The remainder of the paper is structured as follows. Section 2 presents the proposed algorithm for tool path modification to regulate cutting engagement angle, and an illustrating example is demonstrated in the section. Two case studies, carried out experimentally to demonstrate the capability of the proposed approach, are discussed in Sec. 3. Finally the paper concludes with a brief summary as presented in Sec. 4.

2 Proposed Approach

2.1 Algorithm for Tool Path Modification to Regulate Cutting Engagement Angle. Given an initial planar curve representing the desired geometry of the final contour to be machined, and an original contour-parallel (CP) tool path to achieve the desired contour (referred to as the finishing path, hereafter) extracted from NC code, the main aim of the algorithm is to compute the previous tool path trajectory (the path prior to the finishing path) such that the engagement angle can be regulated at a desired level on the machining along the final tool path trajectory (i.e., finishing path). It should be emphasized that this paper focuses on the machining by a straight end mill, and thus, only the two-dimensional interference between a tool and workpiece is considered.

Assume that a trajectory of the tool center location in the finishing path, $\mathbf{o_k}(i) \in R^2(i=1,\ldots,N_k)$, is given by offsetting the final workpiece contour to be machined. As illustrated in Fig. 3, the engagement angle, $\alpha_{en}(i) \in R(i=1,\ldots,N_k)$, is defined by the tool center location, $\mathbf{o_k}(i)$, the intersection point of the tool circumference with the newly generated offset surface, $\mathbf{q_k}(i) \in R^2(i=1,\ldots,N_k)$, and the intersection point of the tool circumference with the semi-finish surface, $\mathbf{p_k}(i) \in R^2(i=1,\ldots,N_k)$. The semi-finish surface, $\mathbf{p_k}(i)$, is generated by the path prior to the finishing path, $\mathbf{o_{k-1}}(i) \in R^2(i=1,\ldots,N_{k-1})$ (referred to as the semi-finish, path hereafter). The intension of the proposed algorithm is to modify the location of the intersection point between the tool circumference and the semi-finish surface, $\mathbf{p_k}(i)$, to the new location $\mathbf{p^*_k}(i)$, in a way such that the cutting engagement angle is modified from $\alpha_{en}(i)$ to its desired value, $\alpha^*_{en}(i)$. Note that the modification of the semi-finish surface, $\mathbf{p_k}(i)$, can be done by the modification of the semi-finish path, $\mathbf{o_{k-1}}(i)$. The new semi-finish

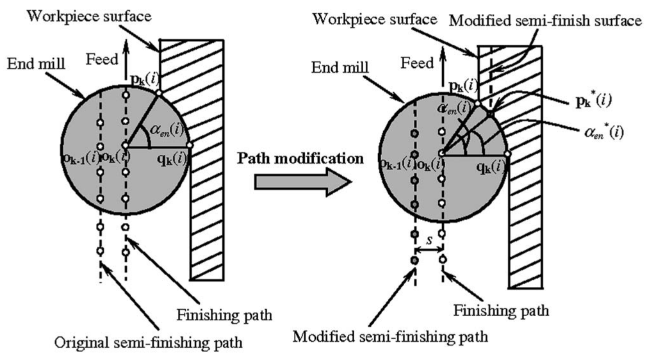

Fig. 3 Concept of the algorithm for tool path modification to regulate cutting engagement angle

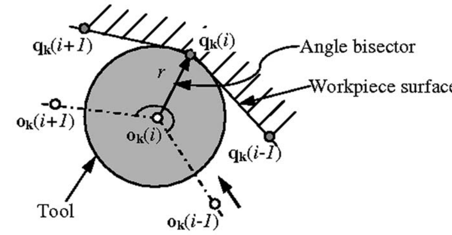

Fig. 4 Parallel offset of the tool center location, $o_k(i)$ by the distance r

path, $\mathbf{o}_{\mathbf{k-1}}^*(i)$, can be given simply by offsetting $\mathbf{p}_{\mathbf{k}}^*(i)$. The detailed algorithm of the computation of new modified offset tool path trajectory, $\mathbf{o}_{\mathbf{k-1}}^*(i)$, can be summarized into the following steps.

Step 1. For the given tool center location of the finishing path, $\mathbf{o}_{\mathbf{k}}(i) \in R^2$ $(i=1,\ldots,N_k)$, compute the intersection point of the tool circumference with the newly generated offset surface, $\mathbf{q}_{\mathbf{k}}(i) \in R^2$ $(i=1,\ldots,N_k)$, by offsetting $o_k(i)$ to the workpiece's side by the tool radius, r. This operation can be written by

$$\mathbf{q}_{\mathbf{k}}(i) = \text{offset}\,[\mathbf{o}_{\mathbf{k}}(i), +r], \quad \text{where} \quad (i = 1, \ldots, N_k) \tag{1}$$

where the function "offset$[\mathbf{o}(i),x]$" represents the computation of the trajectory that is generated by parallel offsetting the trajectory $\mathbf{o}(i)$ by the distance x.

Step 2. Compute the "desired" intersection point of the tool circumference with the semi-finish surface, $\mathbf{p}_{\mathbf{k}}^*(i) \in R^2(i=1,\ldots,N_k)$ such that the engagement angle, $\alpha_{en}(i)$, can be maintained at the desired cutting engagement angle, $\alpha_{en}^*(i)$. In other words, find $\mathbf{p}_{\mathbf{k}}^*(i)$ such that

$$\angle\, \mathbf{p}_{\mathbf{k}}^*(i) \cdot \mathbf{o}_{\mathbf{k}}(i) \cdot \mathbf{q}_{\mathbf{k}}(i) = \alpha_{en}^*(i), \quad \text{and}$$

$$\|\mathbf{p}_{\mathbf{k}}^*(i) - \mathbf{o}_{\mathbf{k}}(i)\| = r, (i = 1, \ldots, N_k)$$

where $\angle$ represents the angle formed by the points, and $\|\cdot\|$ denotes the two-norm of the vector.

Note that $\mathbf{p}_{\mathbf{k}}^*(i) \in R^2$ $(i=1,\ldots,N_k)$ defines the trajectory of modified semi-finish surface (see Fig. 3).

Step 3. Set $i=i+1$ and repeat the steps 1 and 2 until $i=N_k$.

Step 4. Then, by offsetting the modified semi-finish surface trajectory, $\mathbf{p}_{\mathbf{k}}^*(i)$, by the tool radius r, compute the modified tool center trajectory of the semi-finishing path, $\mathbf{o}_{\mathbf{k-1}}(i) \in R^2(i=1,\ldots,N_{k-1})$.

$$\mathbf{o}_{\mathbf{k-1}}(i) = \text{offset}(\mathbf{p}_{\mathbf{k}}^*(i), -r), \quad \text{where} \quad (i = 1, \ldots, N_k) \tag{2}$$

The parallel offset of the location $o(i)$ by the distance x, denoted by offset $[\mathbf{o}(i),x]$, can be computed by shifting $\mathbf{o}(i)$ to the angle bisector direction between the vectors $\mathbf{o}(i)-\mathbf{o}(i-1)$ and $\mathbf{o}(i+1)-\mathbf{o}(i)$ (see Fig. 4). Therefore, note that in the computation of the modified semi-finish path, $\mathbf{o}_{\mathbf{k-1}}(i)$, in Eq. (2), its offsetting direction may not be the same as that in the computation of $\mathbf{q}_{\mathbf{k}}(i)$ in Eq. (1). For the computation of parallel offsets, there have been numerous research efforts to build algorithms with higher robustness and smaller computational complexity [18]. In this paper, we adopt the algorithm developed by Held [19] to compute parallel offsets based on the Voronoi diagram.

The desired engagement angle, $\alpha_{en}^*(i)$, along the final tool path trajectory must be given by considering proper machining conditions for the given tool and the workpiece such that an expected cutting force is maintained all the times. More details will be given in case studies presented in Sec. 3.

2.2 An Illustrating Example. For a more clear understanding of tool path modification by the proposed algorithm, a simple illustrating example on a simple contour consisting of a concave and a convex arc is demonstrated. As can be seen in Fig. 5, both path 1 and path 2 correspond to original contour parallel offset tool paths. Path 1 is applied to semi-finishing while path 2 is a finishing path. By applying the proposed algorithm as illustrated earlier, path 1 is modified into path 1-a such that the cutting engagement with the workpiece along the path 2 is regulated at a desired level. Cutter radius of 5.0 mm and step-over distance (i.e., radial depth of cut) of 1.0 mm are considered for parallel offsetting of tool paths to compute the modified semi-finishing path (path 1-a).

It can be seen from Fig. 5 that, along the concave arc, the semi-finishing path is modified to go "closer" toward the finishing path, which consequently results in smaller cutting engagement with the workpiece in the machining of the finishing path. On the contrary, along the convex arc, the semi-finishing path goes "farther" from the finishing path, indicating a larger cutting engagement in the machining of the finishing path. The resulting action is to regulate the cutting engagement angle always at a desirable level along the final workpiece contour on the machining of the finishing path.

2.3 Remarks. *Remark 1*. It must be emphasized that the proposed tool path modification algorithm focuses on the finishing process by using a straight end mill. In the machining of three-dimensional geometry, the finish path is in many cases executed with a ball or filleted end mill. This may obscure the practical usefulness of the proposed approach. Even in such a case, the authors claim the proposed approach is of a practical value for the following reasons: (i) In die/mold machining, it is often the case

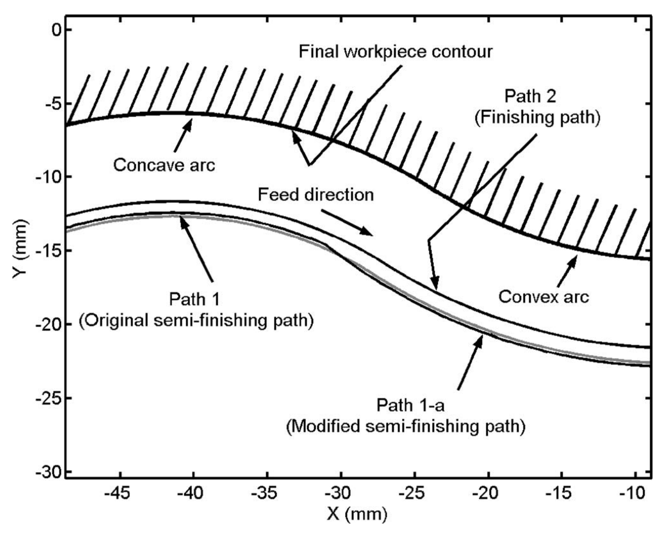

Fig. 5 An illustrating example of tool path modification by the proposed algorithm

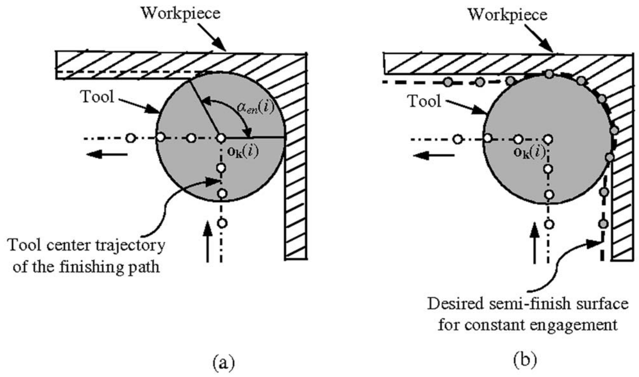

Fig. 6 An illustrative example where constant engagement over the finishing path is not geometrically possible: (*a*) finishing path with a square corner and (*b*) semi-finish surface for constant engagement

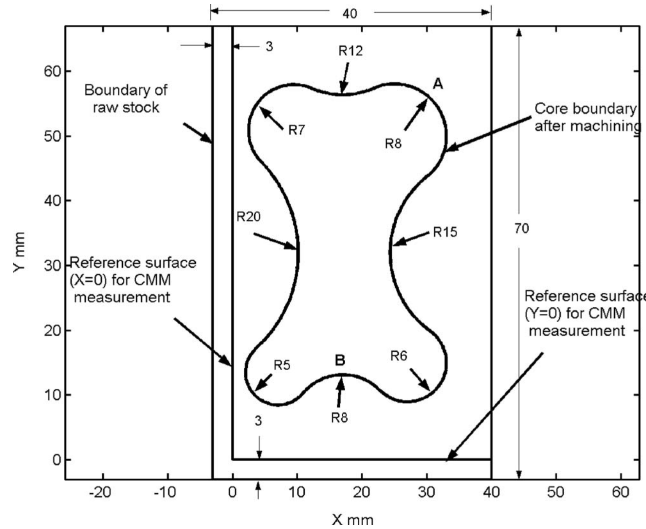

Fig. 7 Geometry of the core contour

that roughing and semi-finish processes are machined by using a straight end mill, followed by a finishing process by using a ball end mill (note that in this paragraph the terms "semi-finish process" and "finishing process" are used in a different meaning from previous sections). Since the radial depth of cut in a ball end mill process is generally very small, when the leftover volume from the semi-finish process significantly varies, it easily causes the variation in the final geometric error of the workpiece surface. By applying the proposed approach to the semi-finishing process by a straight end mill, it can be expected that the semi-finishing process leaves more uniform surface error, which consequently improves the geometric accuracy of the final surface. (ii) The engagement in a ball end mill process is determined by more complex three-dimensional interaction between the tool and the previous workpiece surface, and thus the straightforward extension of the proposed algorithm to a ball end mill process will be difficult. However, when the entire process assumes the 2.5D machining, it is, in practice, reasonable to limit the modification only on the *XY* plane, although in this case the cutting engagement cannot be strictly regulated. In such a case, the algorithm presented in this paper can be extended to a ball end mill process in a straightforward manner.

Remark 2. It must be noted that it is not always possible to generate the modified semi-finish path to regulate the engagement angle at the desired level by using the present approach. For example, when the tool center trajectory of the finishing path contains a square corner as shown in Fig. 6(*a*), the profile of cutting engagement angle, $\alpha_{en}(i)$, has a sudden jump, and becomes discontinuous, near the corner. Geometrically, if the semi-finish surface is given as illustrated in Fig. 6(*b*), the engagement angle can be regulated as constant. It is, however, generally not possible to obtain the semi-finish path that generates this surface. This issue, caused by the discontinuity of the desired semi-finish path, will occur when the finishing path is not smooth. It must be emphasized that the proposed approach can be applied only to a smooth finish path, i.e., the case where the directional difference of the vectors $\mathbf{o}(i)-\mathbf{o}(i-1)$ and $\mathbf{o}(i+1)-\mathbf{o}(i)$ is smaller than some threshold value for any i.

In practical applications, it is often the case that the finishing path contains unsmooth corners. On such a corner, the cutting force, and the consequently the geometric accuracy of the machined surface, are determined dominantly by the feed rate and the machine's contouring error. Under such a condition, it is extremely difficult to determine the "optimal" engagement angle such that the variation in cutting force can be minimized. Therefore, we consider that the regulation of the engagement angle on such an unsmooth corner would not contribute much to the improvement of machining accuracy, and thus that the limited applicability of the present approach is not of a practical importance.

3 Applications of the Proposed Algorithm

In this section, we will present two application examples of the proposed tool path modification scheme to regulate cutting engagement angle. In the proposed scheme, it should be noted that the design of the "desired" engagement angle along the finishing path, $\alpha^*_{en}(i)$, is up to the designer's choice with a consideration on the required geometric accuracy, the surface finish, or the productivity of the finishing. In the first case study, presented in Sec. 3.1, the proposed path modification scheme is applied such that a constant engagement angle is maintained throughout the finishing path, just as the simple example presented in Sec. 2.2. In the second case study, presented in Sec. 3.2, the engagement angle along the finishing path is not regulated at a constant level; it is regulated such that a constant cutting force can be obtained throughout the finishing path, where the feed rate is varied such that a better surface finish can be obtained. The two examples will show that the tool paths generated by the proposed scheme can suppress the variation in the cutting force along the finishing path, under either a constant feed rate or a varying feed rate, which consequently improves the geometric accuracy of the machined workpiece in both cases.

3.1 Case Study I: Constant Cutting Engagement Regulation. In this case study, the proposed algorithm is applied to generate the modified semi-finishing tool path such that a desired constant cutting engagement angle is regulated in the machining along the finishing tool path. Note that the feed rate is kept constant throughout the finish path. The hope with this study is, hence, potentially to regulate a constant cutting force in the finishing tool path (i.e., the final path). The desired cutting engagement angle, α^*_{en}, is determined as follows: assuming the machining along a straight path with the given tool radius r and the step-over distance (i.e., radial depth of cut) s of original contour parallel tool paths, the cutting engagement angle α_{en} is geometrically computed. This value is then used as the desired constant cutting engagement angle α^*_{en} for the tool path modification by the proposed algorithm. In other words, the proposed tool path modification scheme is applied such that the engagement angle along the finishing path does not deviate from the level under which the straight part in the finishing path is cut.

For the purpose of applying the proposed algorithm for path modification, a core contour of different circular arc geometries as shown in Fig. 7 is selected. Figure 8 shows the modified constant

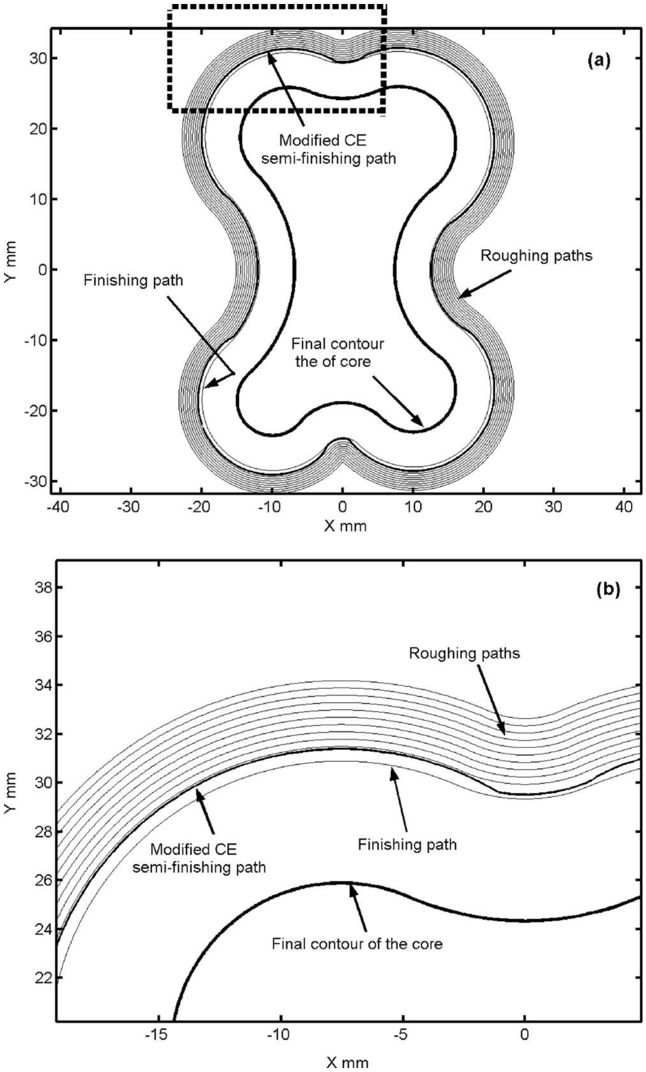

Fig. 8 (*a*) Modified constant engagement (CE) tool path generated by the proposed algorithm (*b*) magnified view of the tool paths in the rectangular box

engagement (CE) tool path generated by the proposed algorithm on the core contour, along with conventional contour parallel paths. First NC programs to produce the final contour of core are generated by commercial CAM software, and the contour parallel finishing offset path is extracted from NC program. Then, by using the proposed algorithm for tool path modification, the modified constant engagement (CE) semi-finishing tool path is generated. The effect of path modification with the desired constant engagement angle on the trajectory of semi-finishing tool path can be noted in the magnified view of tool paths in Fig. 8.

The modified semi-finish path consists of total 1978 line segments of the length 0.1 mm. The computer implementation of the proposed algorithm for tool path modification is carried out by using MATLAB (by Mathworks, Inc.) on a desktop PC of a 2.66 GHz Intel(R) processor. The computation time required from processing the G-code of the finishing path until the generation of the modified CE semi-finishing tool path is less than 1 s.

Figure 9 compares the simulated profiles of engagement angle with an original contour parallel path and the modified CE tool path generated by the proposed algorithm on the finishing path. The computation of engagement angle profiles starts from the circular arc **A** (as marked in Fig. 7) of the core contour while the tool moves in clockwise direction along the contour. It is distinctly

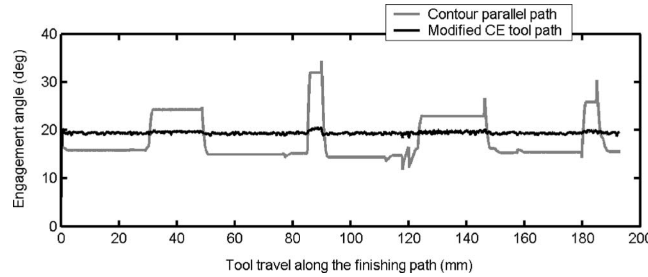

Fig. 9 Engagement angle profiles of an original contour parallel path and the modified CE tool path generated by the proposed algorithm on the finishing path

evident from simulated results that while an original contour parallel path shows a significant variation in engagement angle, the modified CE tool path is able to regulate the engagement angle almost at a desired constant level on the machining of finishing path. Note that small "noise" observed on the engagement angle profile as shown in Fig. 9 could be due to computational errors.

3.1.1 Experiments for Verification. Cutting experiments are conducted to justify the effectiveness of the modified constant engagement (CE) tool path developed by the proposed algorithm. A three-axis vertical high-speed machining center (VCN-410A by Yamazaki Mazak Corp.) is used for machining tests. A core of the geometry shown in Fig. 7 is used as the test workpiece. The detailed cutting conditions used in tests are summarized in Table 1.

For comparison of cutting performance, two machining strategies are adopted. Strategy 1 (contour parallel path) represents the case where conventional contour parallel paths are applied throughout the machining (i.e., from roughing to finishing). Strategy 2 (modified CE tool path) features the case where the proposed modified CE tool path is applied to the semi-finishing path, the path prior to the finishing operation. Note that all the paths except for the semi-finishing path are the same as those in strategy 1. The feed rate is constant throughout on all the roughing and finishing paths.

3.1.2 Results and Discussion. During the machining tests, cutting forces are measured by a dynamometer (Kistler's 9272). In this paper, the cutting force F_{xy} is defined as the resultant vector of cutting force components acting on the tool in X and Y directions (i.e., $\boldsymbol{F}_{xy}=\sqrt{F_x^2+F_y^2}$, where F_x and F_y are cutting force components in X and Y directions, respectively). It must be also noted that all the cutting force profiles presented in this paper are digitally filtered by using a low-pass filter of the cutoff frequency 5 Hz. The profiles show the average of the variation in the cutting force for one rotation of the tool.

Figure 10 depicts a comparison of cutting forces measured during machining of the finishing path for two strategies. It is seen from Fig. 10 that the proposed modified constant engagement

Table 1 Cutting conditions used in experiments

Cutting tool	(Al,Ti)N-coated sintered tungsten carbide Radius end mill Diameter: 10 mm No. of flutes: 6 Tool extension: 35 mm
Workpiece	Hardened steel (JIS SKD 61) with HRc53 Size: 70 mm × 40 mm × 20 mm
Cutting parameters	Spindle speed: 4772 min^{-1} Feed rate: 1200 mm/min Step-over distance: 0.3 mm Axial depth of cut: 5.0 mm
Cutting direction	Down cutting
Coolant	Oil mist

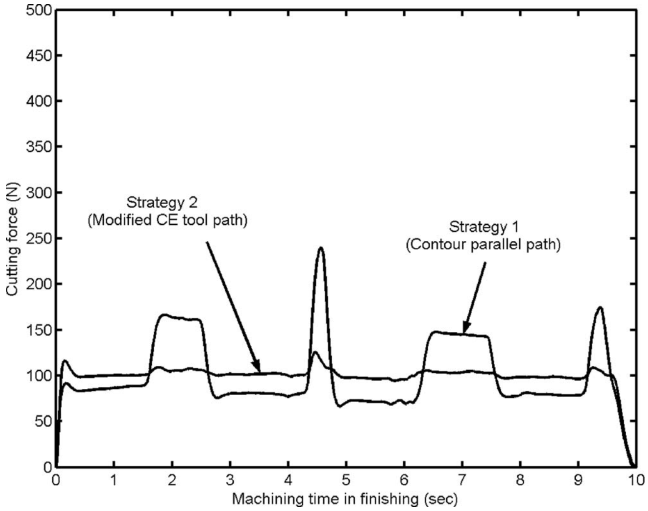

Fig. 10 Comparison of cutting force between contour parallel path and modified CE tool path

(CE) tool path (strategy 2) reveals a reduced variation of cutting force. While comparing to contour parallel path (strategy 1), it reduces maximum variation of cutting force by about 83%.

It is to be noted that since the proposed approach modifies the semi-finish path to regulate cutting engagement in finishing, the variation in cutting force on the semi-finishing will be often larger. Figure 11 compares measured cutting force profiles along the semi-finish path under strategy 1 (contour parallel path) and strategy 2 (modified CE tool path). From Fig. 11, it is found that the variation in cutting force along the semi-finish path is larger in strategy 2. The difference in the cutting force is ~103 N at maximum. From the static stiffness of this tool, the tool deflection caused by the cutting force 103 N is estimated to be ~5.6 μm. Although large variations in the tool deflection on the semi-finish path may potentially change the engagement angle on the finishing path, it can be assumed that the variation in the tool deflection on the semi-finish path is sufficiently small compared to the radial depth of cut on the finishing path. The fact that the variation in the cutting force on the finishing path is significantly suppressed in strategy 2 (as shown in Fig. 10) shows the validity of this assumption in this experiment.

Figure 12 shows geometric error profiles of the machined sur-

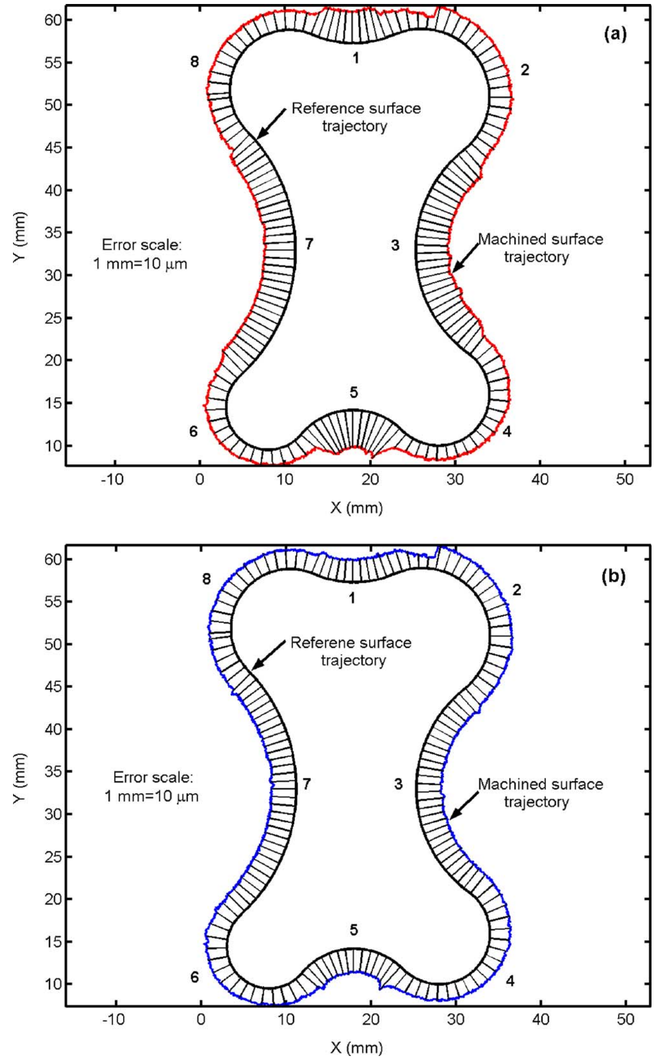

Fig. 12 Machined surface profiles with respect to reference surface of core workpiece measured by the CMM: (*a*) contour parallel path (strategy 1) and (*b*) modified constant engagement (CE) tool path (strategy 2)

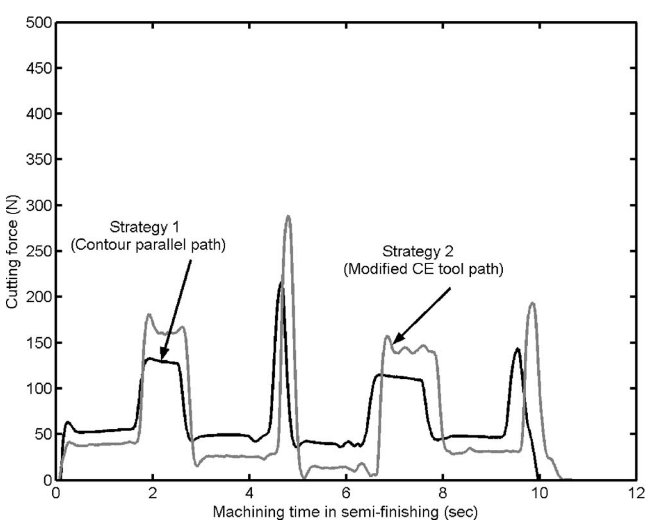

Fig. 11 Measured cutting force profiles along the semi-finishing path

face with respect to reference surface trajectory measured by a coordinate measuring machine (CMM) (UPMC 850 by Carl Zeiss Inc.). The geometric error (i.e., machined surface error) can be defined as the normal distance between the machined surface trajectory and the reference (i.e., nominal) surface trajectory. For a clear comparison, the same error profiles drawn from Fig. 12 with the distance along the reference surface from the starting point indicated by "**8**" are shown in Fig. 13. From Figs. 12 and 13, it can be revealed that by applying modified CE tool path (strategy 2), the variation of machined surface error is significantly reduced, when compared to that in contour parallel tool path (strategy 1). The maximum variation of machined surface error is reduced by 75%. In this study, the maximum machined surface error variation is defined as the difference between the maximum machined surface error (i.e., peak of the error profile) and the minimum machined surface error (i.e., valley of the error profile).

The mean values of machined surface error for each of eight corners along the core contour are presented in Fig. 14. From Fig. 14, it is evident that by applying modified CE tool path, a significant reduction of mean machined surface error is observed especially at concave circular arcs, indicating an overall uniform error level along the contour of machined workpiece.

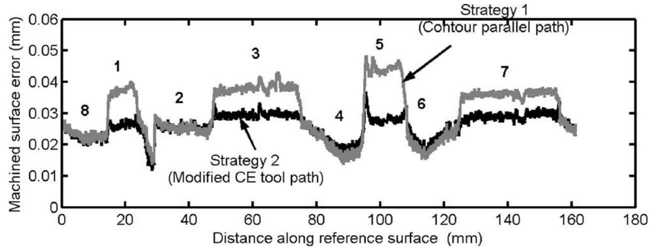

Fig. 13 Machined surface geometric error profiles with distance along reference surface of the core workpiece (the numbers on top of graphs correspond to the corner names, same as those indicated in Fig. 12)

3.2 Case Study 2: Constant Cutting Force Regulation With Constant Feed Rate at Cutting Point. In case study 1, the proposed tool path modification scheme is applied such that the engagement angle is kept constant throughout the finishing path, which consequently regulates the cutting force constant when the finishing path is machined under a constant feedrate. Case study 2 shows that the proposed tool path generation scheme can be applied such that the finishing path is subject to a constant cutting force even when the feed rate is scheduled to given profile. As a simple example of such a feed-rate regulation scheme, we consider the following case.

3.2.1 Overview. In 2.5D contour machining, the feed rate at the actual cutting point varies even when the feed rate at the tool center is kept constant. The variation in feed per tooth at the cutting point naturally causes the variation in the width of cutter marks generated on the machined surface, which often deteriorates the surface quality. To address it, a scheme to regulate the feed rate at tool center such that the feed rate at the cutting point is kept constant has been well known [20], and it is implemented in some latest commercial CAM software. The idea is that by maintaining the feed rate at the cutting point constant, the width of cutter marks on the machined surface will be ideally constant, which potentially will contribute to the improvement of the surface quality. However, a constant feed rate at the cutting point generally does not keep the cutting force constant. Then, by applying the proposed algorithm as illustrated earlier, the semi-finishing path is modified with an optimized cutting engagement angle such that an expected cutting force is regulated efficiently in the finishing path. By applying both the feed-rate optimization and the tool path modification, it can be expected that both the geometric accuracy and the surface quality of the machined workpiece will be improved.

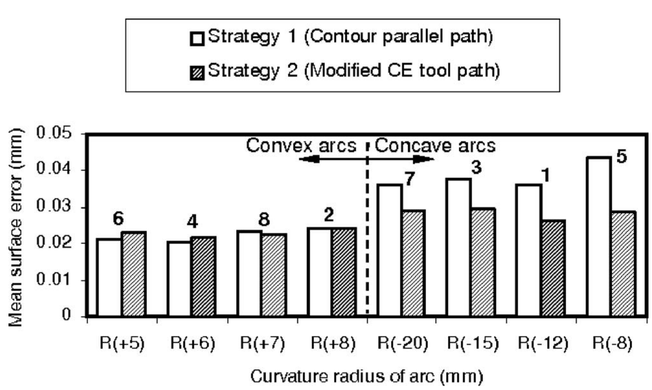

Fig. 14 Mean surface geometric error profiles with respect to curvature radius of core workpiece (*R* (+): convex arc, *R* (−): concave arc; the numbers on top of graphs correspond to the corner names, same as those indicated in Fig. 12)

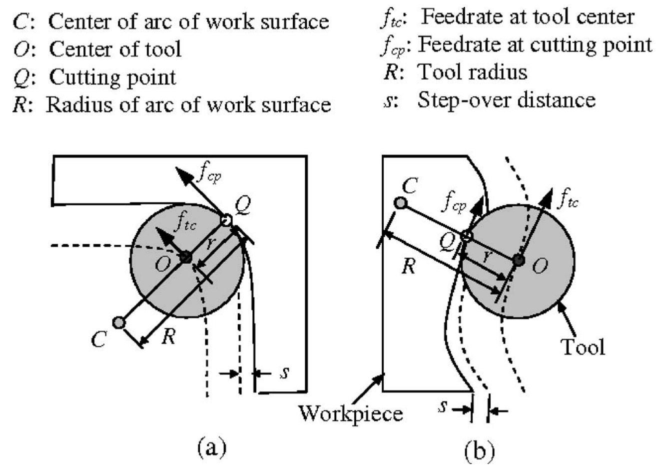

Fig. 15 Definition of feedrate at the cutting point and feedrate at tool the center in 2.5D contour milling: (*a*) concave arc milling and (*b*) convex arc milling

3.2.2 Definition of Feed Rate at the Cutting Point and its Regulation. Figure 15 defines the feedrate at the cutting point and the feed rate at the tool center for concave and convex arc milling. From Fig. 15, it can be easily understood that feed rate at the cutting point f_{cp} is totally different from that at the tool center f_{tc}, depending on the geometry of workpiece contour. Hence, in order to keep the feed rate at the cutting point f_{cp} at a constant level, we have varied the feed rate at the tool center f_{tc}. Assume that the geometry of workpiece contour such as curvature radius, $R(i)$ ($i=1,\ldots,N_k$), along the trajectory of the finishing path, $\mathbf{o_k}(i) \in R^2(i=1,\ldots,N_k)$, is given. Thus, variable feed-rate at the tool center, $f_{tc}^*(i)$ ($i=1,\ldots,N_k$) can be optimized as follows:

$$\text{For concave arc,} \quad f_{tc}^*(i) = \frac{f_{cp}(R(i)-r)}{R(i)} \tag{3}$$

$$\text{For convex arc,} \quad f_{tc}^*(i) = \frac{f_{cp}(R(i)+r)}{R(i)} \tag{4}$$

where r is the tool radius. The desired feed rate at the cutting point f_{cp} is chosen from the machining database or recommended by the industry.

3.2.3 Optimization of Cutting Engagement Angle for Constant Cutting Force Regulation. As is mentioned earlier, a constant feed rate at the cutting point does not necessarily keep the cutting force at a constant value. However, in contour machining, regulating cutting force at a desired level is an important concern to reduce the tool deflection and thus to enhance the machining accuracy.

When the feed rate along the finishing tool path trajectory is given by $f_{tc}^*(i)$ ($i=1,\ldots,N_k$), first a profile of the desired engagement angle is computed such that the cutting force is regulated at the given desired level. We here assume that a kinematic model to predict the cutting force from given cutting conditions is available, on which the computation of the desired engagement angle is based. In this study, we adopt the cutting force prediction model developed by Otsuka et al. [21]. When the feed rate at the cutting point is given, Otsuka's cutting force model can be rewritten as

$$\hat{F} = \beta_0 + \beta_1 \sin\alpha_{en}(i) + \beta_2\alpha_{en}(i) + \beta_3[\sin\alpha_{en}(i)]^2 + \beta_4[\alpha_{en}(i)]^2 + \beta_5\alpha_{en}(i)\sin\alpha_{en}(i) \tag{5}$$

where $\hat{F}$ denotes the predicted cutting force, and β_0, β_1, β_2, β_3, β_4, and β_5 are constant coefficients which must be identified in advance for the given tool and the workpiece by cutting experi-

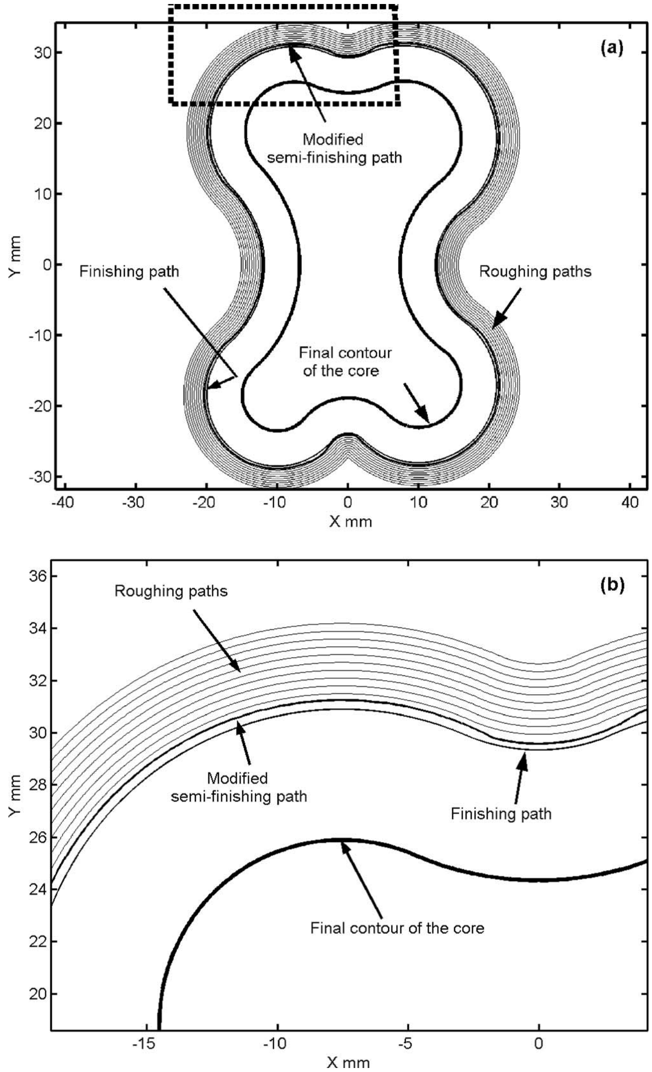

Fig. 16 (*a*) Modified semi-finishing tool path generated by the proposed algorithm with optimized cutting engagement angle and (*b*) magnified view of the tool paths in the rectangular box

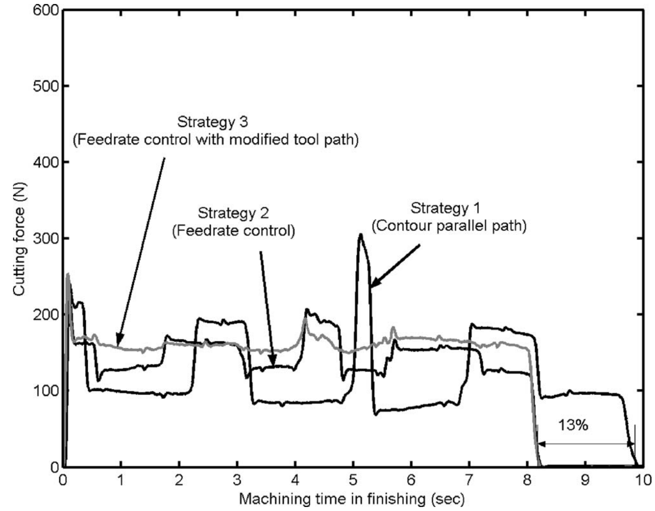

Fig. 17 Comparison of cutting forces in finishing

ments as shown in [21]. As Eq. (5) is a nonlinear equation, a trust-region method for nonlinear optimization [22] is adopted to solve the above equation to obtain a profile of the optimized cutting engagement angle, $\alpha^*_{en}(i)$ $(i=1,\ldots,N_k)$ along the tool path trajectory for the given desired cutting force level.

3.2.4 Tool Path Modification With Optimized Cutting Engagement Angle. Now, using the proposed algorithm for tool path modification as described in Sec. 2, the trajectory of modified semi-finishing path, $\mathbf{o_{k-1}}(i) \in R^2(i=1,\ldots,N_{k-1})$ is generated such that the cutting engagement angle is maintained at $\alpha^*_{en}(i)$ along the trajectory of finishing path, $\mathbf{o_k}(i) \in R^2(i=1,\ldots,N_k)$.

Figure 16 shows the modified semi-finishing path generated by the current proposed algorithm, along with the finishing path on the same core workpiece contour (see Fig. 7), and the effect of path modification on the trajectory of semi-finishing path can be noted in the magnified view of Fig. 16. To be noted again is that, in the machining along the finishing path trajectory, the optimized variable feed rate at the tool center $f^*_{tc}(i)$, is maintained to keep constant feedrate at the cutting point.

3.2.5 Experiments for Verification. Machining experiments on the same core workpiece are carried out in order to verify the significance of the proposed approach. A three-axis vertical machining center (Mori Seiki GV503) is used in cutting tests. Cutting conditions used during the experiments are same as shown in Table 1 except for the axial depth of cut. In this experiment, the axial depth of cut of 5.24 mm is maintained throughout.

Three machining strategies are adopted in this case study. Strategy 1 (contour parallel path) represents the case where contour parallel tools with a constant feed rate of 1200 mm/min are applied throughout the machining (i.e., from roughing to finishing). Strategy 2 (feed-rate control) is the case where a contour parallel tool path with variable feed rate at tool center is applied to the finishing in order to keep a constant feed rate of 1200 mm/min at the actual cutting point. As computed by using Eqs. (3) and (4) for the geometry of the core contour, the variable feed rate at the tool center in the finishing path ranges from 450 mm/min to 2400 mm/min. Note that in strategy 2, the semi-finishing path is the same as the original contour parallel path. Finally, strategy 3 (feed-rate control with modified tool path) designates the case where the tool path modification by the proposed algorithm is applied to the semi-finishing while a contour parallel tool path with variable feed rate at tool center (as same in strategy 2) is applied to the finishing.

3.2.6 Results and Discussion. Figure 17 illustrates a comparison of cutting forces measured by a dynamometer (Kistler's 9257B) in finishing. The definition of cutting forces measured in the cutting tests for this case study is as same as that described in Sec. 3.1.2. From Fig. 17, it is seen that contour parallel path (strategy 1) shows a drastic variation of cutting force. A cutting test under a feed-rate control with keeping a constant feed rate at the cutting point (strategy 2) also reveals a variation of cutting force. However, machining under a feed-rate control with a modified tool path generated by the proposed algorithm (strategy 3) reduces the variation of cutting force by about 80% and 44% (at maximum) while comparing to those under strategies 1 and 2, respectively. In addition, strategies 2 and 3 improve cutting time by ~13% with respect to that in strategy 1 due to the feed-rate control. Note that, in Fig. 17, there is a little jump of cutting forces at the beginning of the cut for all the cases. This can be attributed to the fact that at the beginning of cut, the tool approaches to the workpiece in a direction perpendicular to the contour, which causes a sudden rise in cutting force since the tool undergoes the full immersion cutting there for a short time. This process is ignored in all the strategies.

Figure 18 shows profiles of commanded and measured feed rate on the machining of finishing path under strategies 2 and 3. It indicates that, in actual machining, the commanded variable feed rate at tool center to keep a constant feed rate at the cutting point

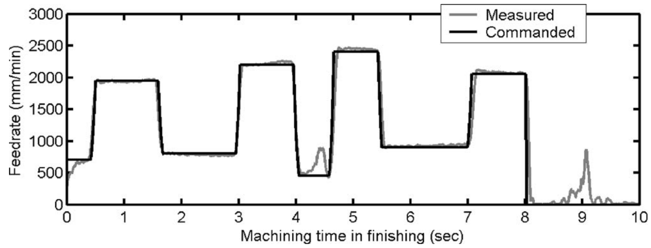

Fig. 18 Profiles of measured and commanded feedrate in finishing under strategy 2 (feed-rate control)

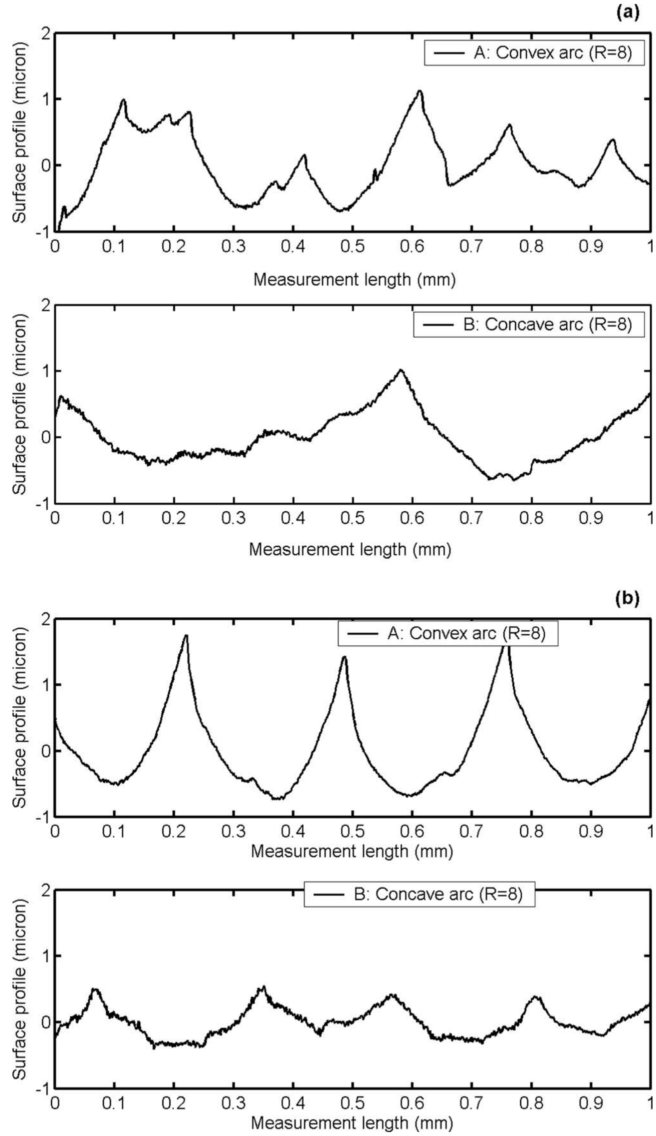

Fig. 19 Cutter mark profiles of a convex arc (marked by A in Fig. 7) and a concave arc (marked by B in Fig. 7) of curvature radius of 8 mm of machined core workpiece: (*a*) contour parallel path (strategy 1) and (*b*) feedrate control with modified tool path (strategy 3)

is regulated almost appropriately by the servocontroller of the machine tool. In this experiment, the measured feed rate profile is given through linear encoders on *X* and *Y* directional feed drives.

Surface profiles of machined core workpiece are measured by a contour form measurement system (Mitsutoyo's SV-C500). Measurements of surface profiles are taken at ~2.6 mm depth from the top face of the core workpiece in the axial direction (i.e., about half of the axial depth of cut). Surface measurement results shown in Fig. 19(*a*) indicate that, in the machining under contour parallel path with constant feed rate at the tool center (strategy 1), cutting marks are dense at convex arc as marked by **A** in Fig. 7, while they are wide at concave arc as marked by **B** in Fig. 7. In contrary, in the cutting under the feed-rate control with modified tool path (strategy 3), cutting marks are likely to span more evenly at both convex and concave arcs (Fig. 19(*b*)). This result manifests that, when the feed rate at the tool center is constant, and thus, the feed rate at the cutting point varies depending on the geometry of the tool path (strategy 1), the density of cutter marks varies significantly. By keeping constant feed rate at the cutting point (strategy 3), the surface quality can be improved. Note that in Fig. 19(*b*), the amplitude of cutting mark peaks on the convex arc (**A**) is slightly larger in strategy 3 than that in strategy 1. This might happen because the average cutting force on the convex arc (**A**) is larger in strategy 3 than that in strategy 1 due to the feed-rate control.

Machined surface trajectories of the core workpiece measured by a CMM (Leitz's PMM 866) are shown in Fig. 20. Figure 21 describes machined surface geometric error profiles with respect to the distance along the reference surface in the finishing. From Figs. 20 and 21, it is seen that, in the machining under feed-rate control with the modified tool path (strategy 3), machined surface geometric error is more constant along the reference trajectory of the core workpiece while comparing with those under strategies 1 and 2. Neglecting larger error at entry/exit points of the cutting near the point **1**, the feed-rate control with the modified tool path (strategy 3) reduces the maximum machined surface error variation by ~57.5% and ~19.3% compared to those under the conventional contour parallel path (strategy 1) and the feedrate control (strategy 2) respectively.

Note that in Fig. 21, it can be observed that the machining under contour parallel path (strategy 1) produces the least machined surface error on convex arcs. The intention of applying the modified semi-finish path (and the feed-rate control) is to reduce the variation in the cutting force over the entire finishing path, which leads to the *increase* of cutting force at convex arcs (see also Fig. 17). This naturally results in larger tool deflection and, consequently, larger machined surface error at convex arcs. In this study, we are more interested in obtaining the least variation of machined surface error (i.e., uniform geometric surface) over the entire finishing surface. In strategy 3, the semi-finish path and the feed rate are modified such that the cutting force at convex arcs is increased, and that at concave arcs is decreased.

The mean values of machined surface geometric error for each of eight corners of the core contour are drawn in Fig. 22. Results from Fig. 22 verify more uniform geometric error achieved under the feed-rate control with the modified tool path developed by the proposed algorithm.

4 Conclusions

The following can be concluded from this study:

(a) Although conventional contour parallel tool paths offer varying cutting engagement, this paper proposes an algorithm to generate a new offset tool path, which regulates the cutting engagement angle at a desired value in the two-dimensional contour machining by using a straight end mill.

(b) In an attempt to signify the capability of the proposed algorithm, two case studies are demonstrated. From the first case study, it has been shown that the modified constant engagement (CE) tool path generated by the proposed algorithm is able to regulate the cutting engagement at a desirable constant level, which results in an

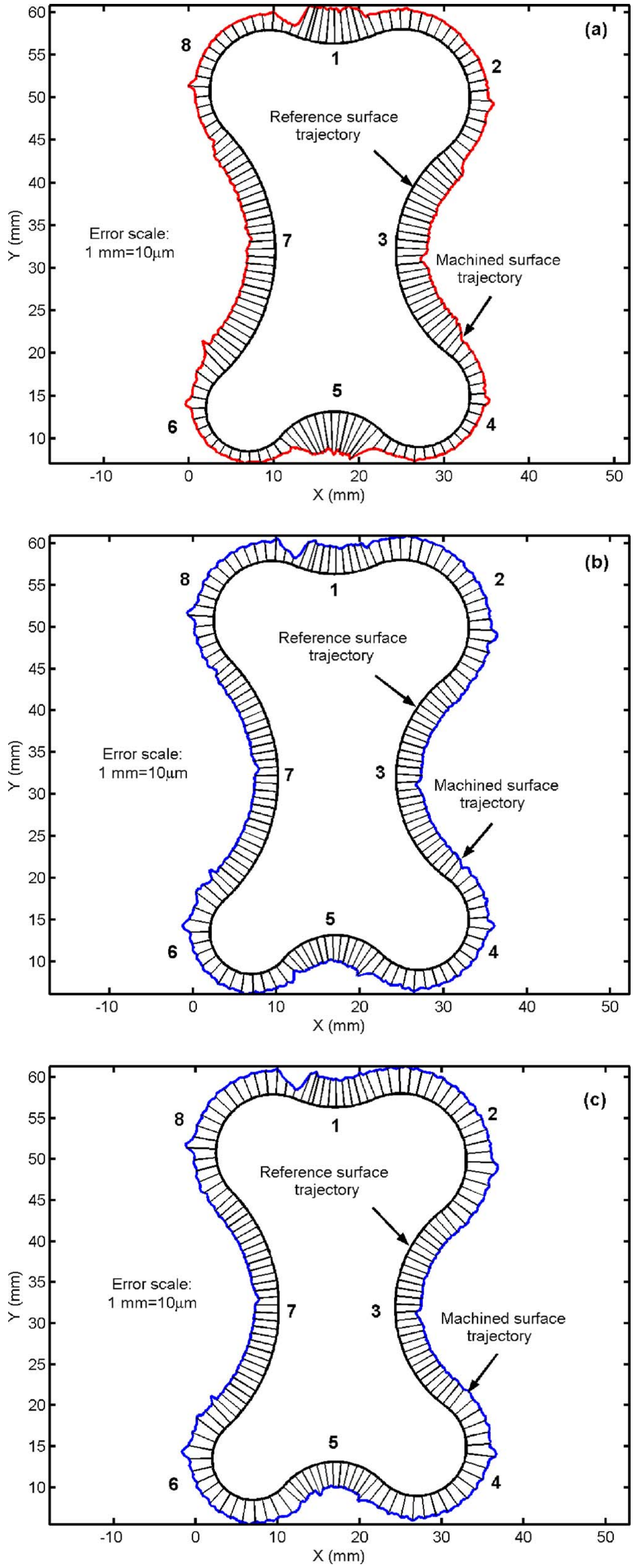

Fig. 20 Machined surface trajectories with respect to the reference surface of core workpiece: (*a*) contour parallel path (strategy 1), (*b*) feed-rate control (strategy 2), and (*c*) feed-rate control with modified tool path (strategy 3)

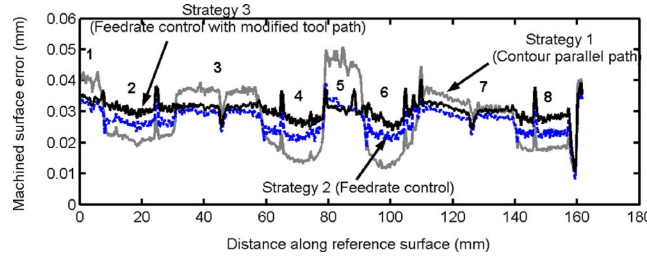

Fig. 21 Machined surface geometric error profiles with distance along reference surface of core workpiece (the numbers on top of graphs correspond to the corner names, same as those indicated in Fig. 20)

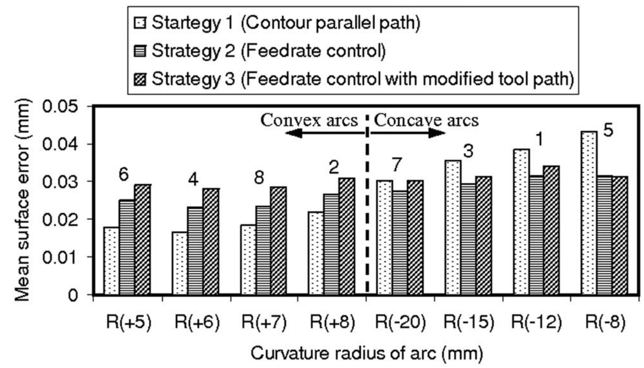

Fig. 22 Mean surface geometric error profiles with respect to curvature radius of core workpiece (*R*(+): convex arc, *R*(−): concave arc; the numbers on top of graphs correspond to the corner names, same as those indicated in Fig. 20)

83% reduction of the maximum variation of cutting force while comparing to that for the conventional contour parallel tool path. Consequently, in terms of geometric accuracy, it reveals a 75% reduction of the variation in the machined surface error compared to that for the contour parallel path.

(c) The second case study demonstrates the capability of the proposed algorithm when it is applied to a feed-rate control scheme where the feed rate at the tool center is varied to keep a constant feed rate at the cutting point. Although a constant feed rate at the cutting point does not regulate constant cutting force, it has been shown that by applying the modified tool path generated by the proposed algorithm, a desired cutting force can be maintained more accurately and efficiently, and hence, the variation in the machined surface geometric error is reduced and the surface quality is improved. Results from experimental verification of the proposed approach, include far-reduced variation of cutting forces, uniform cutting marks on the machined surface, and consequently, an improved geometric accuracy of the machined contour.

Acknowledgment

This research is partially funded by Advanced Machining Technology and Development Association. We also sincerely acknowledge the cooperation from Okuma Corporation and Kyoto Prefectural Technology Center for Small and Medium Enterprises in CMM measurements presented in this paper. The machining center used in the experiments presented in Sec. 3.2 is supported by the Machine Tool Technologies Research Foundation via Equipment on Loan Award Program.

References

[1] Kline, W.A., Devor, R.E., and Lindberg, J., 1982, “Prediction of Cutting Forces in End Milling With Application to Cornering Cuts,” Int. J. Mach. Tool

Des. Res., **22**, pp. 7–22.
[2] Kramer, T.R., 1992, "Pocket Milling With Tool Engagement Detection," J. Manuf. Syst., **11**(2), pp. 114–123.
[3] Choy, H.S., and Chan, K.W., 2003, "Modeling Cutter Swept Angle at Cornering Cut," Int. J. CAD/CAM, **3**(1), 1–12.
[4] Tlusty, J., Smith, S., and Zamudio, C., 1990, "New NC Routines for Quality in Milling," CIRP Ann., **39**(1), pp. 517–521.
[5] Smith, S., Cheng, E., and Zamudio, C., 1991, "Computer-Aided Generation of Optimum Chatter-Free Pockets," Int. J. Mater. Prod. Technol., **28**, pp. 275–283.
[6] Fussel, B.K., and Srinivasan, K., 1989, "On-Line Identification of End Milling Process Parameters," ASME J. Eng. Ind., **111**, pp. 322–330.
[7] Asai, A., and Tsuruhashi, T., 1988, "Development of Die-Cutting Feedrate Control System," JSAE Rev., **9**, pp. 72–82.
[8] Rehorn, A.G., Jiang, J., and Orban, P.E., 2005, "State-of-the-Art Methods and Results in Tool Condition Monitoring: A Review," Int. J. Adv. Manuf. Technol., **26**, pp. 693–710.
[9] Spence, A.D., and Altintas, Y., 1994, "A Solid Modeler Based Milling Process Simulation and Planning System," ASME J. Eng. Ind., **116**, pp. 61–69.
[10] Fussel, B.K., Jerard, R.B., and Hemmet, J.G., 2001, "Robust Feedrate Selection for 3-Axis NC Machining Using Discrete Models," ASME J. Manuf. Sci. Eng., **123**, pp. 214–224.
[11] Bae, S.H., Ko, K., Kim, B.H., and Choi, B.K., 2003, "Automatic Feedrate Adjustment for Pocket Machining," Comput.-Aided Des., **35**, pp. 495–500.
[12] Iwabe, H., Fuji, Y., Saito, K., and Kishinami, T., 1989, "Study on Corner Cut by End Mill Analysis of Cutting Mechanism and New Cutting Method at Inside Corner," J. Jpn. Soc. Precis. Eng., **99**(5), pp. 841–846.
[13] Tsai, M.D., Takata, S., Inui, M., Kimura, F., and SataT., 1991, "Operation Planning Based on Cutting Process Models," CIRP Ann., **40**(1), pp. 95–98.
[14] Choy, H.S., and Chan, K.W., 2003, "A Corner-looping Based Tool Path for Pocket Milling" Comput.-Aided Des., **35**, pp. 155–166.
[15] Kim, H.C., Lee, S.G., and Yang, M.Y., 2006, "An Optimized Contour Parallel Tool Path for 2D Milling With Flat End Mill," Adv. Manuf. Technol., **31**(5-6), pp. 567–573.
[16] Stori, J.A., and Wright, P.K., 2000, "Constant Engagement Tool Path Generation for Convex Geometries," J. Manuf. Syst., **19**(3), pp. 172–184.
[17] Wang, H., Jang, P., and Stori, J.A., 2005, "A Metric-Based Approach to Two-Dimensional (2D) Tool-Path Optimization for High-Speed Machining," ASME J. Manuf. Sci. Eng., **127**(1), pp. 33–48.
[18] Dragomatz, D., and Mann, S., 1997, "A Classified Bibliography of Literature on NC Milling Path Generation," Comput.-Aided Des., **29**(3), pp. 239–247.
[19] Held, M., 2001, "VRONI: An Engineering Approach to the Reliable and Efficient Computation of Voronoi Diagrams of Points and Line Segments," Comput. Geom., **18**(2), pp. 95–123.
[20] Nishida, S., Ohtsuka, H., Yamaji, I., Kakino, Y., Ibaraki, S., and Matsubara, A., 2004, "The Improvement of Productivity and Quality of Die/Mold by Constant Feedrate Control at the Cutting Point," *Proc. of 2004 Japan-USA Symposium on Flexible Automation (JUSFA'2004)*, Denver, July 19–21.
[21] Otsuka, H., Kakino, A., Matsubara, A., Nakagawa, H., and Hirogaki, T., 2001, "A Study on Endmilling of Hardened Steel (2nd Report)–Control for Constant Cutting Forces in Corner Profile Endmilling Including Connection Areas of Tool Paths," J. Jpn. Soc. Precis. Eng., **67**(8), pp. 1294–1298.
[22] Byrd, R. H., Schnabel, R. B., and Shultz, G. A., 1988, "Approximate Solution of the Trust Region Problem by Minimization Over Two-dimensional Subspace," Math. Program., **67**(2), pp. 247–263.